KINETIC MODELLING AND REACTOR SIMULATION FOR METHANOL SYNTHESIS FROM HYDROGEN AND CARBON MONOXIDE ON A COPPER-BASE CATALYST

Kyu Sung Lee, Chang Shik Hong, and Chai-sung Lee*

Department of Chemical Engineering, College of Engineering, Seoul National University, Seoul, Korea

(Receives 10 August 1983 • accepted 25 September 1983)

Abstract—Some hypothesized reaction mechanisms were tested out against the supplied experimental data on methanol synthesis from syn gas on copper-based catalyst at different temperatures. Each reaction mechanism consists of three to five intermediate steps, one of which being inevitably the rate determining step for overall reaction $CO + 2H_2 = CH_3OH$. It was concluded from these tests that the reaction between the adsorbed reactants on the catalyst seemed to be the rate determining step when diffusion resistance was assumed to be negligible.

Once the rate determining step is known, the rate equation can be derived, and the modelling of an actual reactor is relatively a routine procedure including the setting up of mass, momentum, and energy balance equations assuming necessary conditions. As the result of simulation, plots of component concentration, reaction rate, temperature, and pressure profiles against reactor length and a table of summary were presented.

INTRODUCTION

It was pointed out by Nishtala et al.[1] that the kinetics of methanol synthesis on copper-based catalyst was not clearly understood. It was by them that some exploratory experimental work was performed on this subject. They concluded that pore diffusion was a limiting factor giving rise to an empirical equation for the rate of methanol synthesis which included the effectiveness factor represented by the reciprocal of Thiele modulus. However, the diffusional resistance, either of surface film or of pore, was completely neglected in this work to comply with the directives set out by the organizing committee of the workshop. Under this circumstance, the reaction rate can not be controlled by other than the slowest step in the intermediate reactions that were hypothesized to take place in the course of reaching to the final product. This simplification alleviate greatly the work of search for the rate determining factor beyond the regime of chemical reaction. It appears, therefore, more feasible than otherwise to name which one of the hypothesized reaction mechanisms is the most plausible. Once the reaction mechanism and the corresponding rate expression are found, simulation of reactor performance can immediately be carried out.

The type of reactor we have to deal with is a simple, one-dimensional, plug-flow, pseudo-homogeneous, non-isothermal reactor as designated by the workshop organizers in compromise with the actual reactor behavior. Among others, greater simplicity is obtained by the pseudo-homogenity of the catalyst bed reaction which otherwise has to be treated as a distributed parameter system.

Now it will be necessary to reenumerate the given data for our kinetic analyses, the reactor, catalyst, and the process conditions as well as physical properties and thermodynamic information in Table 1, 2, and 3. It should be clearly understood that all the following work is based on these data.

KINETIC ANALYSIS

The overall reaction between carbon monoxide and hydrogen is assumed to be a simple methanol forming reaction without side reactions as shown below:

$$CO+2H_2=CH_3OH \quad (1)$$

This reaction is rewritten, for further simplicity, as follows:

$$A+2B\rightleftharpoons R \quad (2)$$

* To whom correspondence should be directed.

Table 1. Data for Kinetic Analysis*

Expt.	Rate** mol/m³/s	Temp. °K	Partial Pressure, kPa Methanol	CO	Hydrogen
A	6.753	495	1013	4052	8509
B	4.819	495	1013	4052	5906
C	6.270	495	1013	1530	8509
D	4.928	495	1013	1530	5906
E	10.115	495	253	4052	8509
F	7.585	495	253	4052	5906
G	9.393	495	253	1530	8509
H	7.124	495	253	1530	5906
I	1.768	475	1013	4052	8509
J	1.177	475	1013	4052	5906
K	1.621	475	1013	1530	8509
L	1.293	475	1013	1530	5906
M	2.827	475	253	4052	8509
N	2.125	475	253	4052	5906
O	2.883	475	253	1530	8509
P	2.035	475	253	1530	5906
CP1	4.030	485	507	2533	7091
CP2	3.925	485	507	2533	7091
CP3	3.938	485	507	2533	7091
AA	10.561	500	507	2533	7091
BB	1.396	470	507	2533	7091
CC	2.452	485	1520	2533	7091
DD	5.252	485	172	2533	7091
EE	3.731	485	507	4862	7091
FF	3.599	485	507	1276	7091
GG	5.085	485	507	2533	9330
HH	3.202	485	507	2533	5369

letting, A, B, and R to represent CO, H_2, and CH_3OH, respectively. But, when this reaction is carried out on a catalyst, its surface interaction with the reactant and resultant at the active sites, and the subsequent chemical combinations must be considered. The interaction includes both adsorption and desorption. One possible mechanism of yielding R from A and B on a catalyst may be written as follows:

$$A + L \underset{k'_A}{\overset{k_A}{\rightleftharpoons}} A^* \tag{3a}$$

$$2B + 2L \underset{k'_B}{\overset{k_B}{\rightleftharpoons}} 2B^* \tag{3b}$$

$$A^* + 2B^* \underset{k'_S}{\overset{k_S}{\rightleftharpoons}} R^* + 2L \tag{3c}$$

$$R^* \underset{k_R}{\overset{k'_R}{\rightleftharpoons}} R + L \tag{3d}$$

where k and k′ are the rate constants for forward and backward reactions, subscript S means surface reaction, and superscript * means activated state. References were made to the previous works[2,3,4].

In this mechanism, either one of the four steps can be the rate determining step provided that the choice does not contradict with the experimentally confirmed data in Table 1. In order to determine the rate controll-

* Private communication from Professor J.M. Berty, et al of the Department of Chemical Engineering, The University of Akron, February, 1983.

** Rates are mols methanol formed per cubic meter of catalyst-packed reactor volume per second

Table 2. Reactor, Catalyst, and Process Conditions for Simulation

Reactor Description

Type :	Shell and tube
Tubes :	3000, 38.1 mm I.D. x 12 m
Coolant :	Boiling water on shell-side.
	Assume coolant temperature constant at 483°K
Overall Heat-Transfer Coefficient :	Assume 631 watts/m²/K

Catalyst Description

Shape :	Approximately spherical
Diameter :	7.87 mm
Effective Catalyst Bed Void Fraction :	0.40
Diffusional Resistance :	May be ignored

Process Conditions

Feed-Gas :	Composition: 70 mol percent H_2
	30 mol percent CO
	Space-Velocity: 10000 Standard cubic meter per hour/m³ reactor volume
Reactor Inlet Pressure :	10.13 MPa
Reactor Inlet Temperature :	473°K
Reactor Coolant Temperature :	483°K (constant)

Note: Investigate the effect of different coolant temperatures

Table 3. Physical Properties and Thermodynamic Information

Prandtl Number of Gas :	0.70 (Assume constant)
Heat Capacity of Gas :	29.31 J/mol/°K (Assume constant)
Viscosity of Gas :	1.6×10^{-5} Pa.s (Assume constant)
Heat of Reaction :	-97.97 kJ/mol methanol formed
Thermodynamic Equilibrium Constant :	$\mathrm{Log}_{10}K=\frac{3921}{T}-7.971\mathrm{Log}_{10}T+0.002499T-2.953(10^{-7})T^2+10.2$ (Dimensionless and T is in °K)

Note: In all calculations assume that ideal gas law applies.

Table. 4. Reaction Mechanisms and Their Intermediate Steps for Reaction: $A+2B\rightleftharpoons R$

	a	a	c	d	e
I	$A+L\underset{k'_B}{\overset{k_A}{\rightleftharpoons}}A^*$	$2B+2L\underset{k'_B}{\overset{k_B}{\rightleftharpoons}}2B^*$	$A^*+2B^*\underset{k'_S}{\overset{k_S}{\rightleftharpoons}}R^*+2L$	$R^*\underset{k_R}{\overset{k'_R}{\rightleftharpoons}}R+L$	
II	$A+L\underset{k'_A}{\overset{k_A}{\rightleftharpoons}}A^*$	$2H_2+4L\underset{k'_H}{\overset{k_H}{\rightleftharpoons}}4H^*$	$A^*+4H^*\underset{k'_S}{\overset{k_S}{\rightleftharpoons}}R^*+4L$	$R^*\underset{k'_S}{\overset{k'_R}{\rightleftharpoons}}R+L$	
III	$2H_2+4L\underset{k'_H}{\overset{k_H}{\rightleftharpoons}}4H^*$	$A+2H^*\underset{k'_D}{\overset{k_D}{\rightleftharpoons}}D^*+L$	$D^*+2H^*\underset{k'_S}{\overset{k_S}{\rightleftharpoons}}R^*+2L$	$R^*\underset{k_R}{\overset{k'_R}{\rightleftharpoons}}R+L$	
IV	$2H_2+4L\underset{k'_H}{\overset{k_H}{\rightleftharpoons}}4H^*$	$A+4H^*\underset{k'_S}{\overset{k_S}{\rightleftharpoons}}R^*+3L$	$R^*\underset{k_R}{\overset{k'_R}{\rightleftharpoons}}R+L$		
V	$2B+2L\underset{k'_B}{\overset{k_B}{\rightleftharpoons}}2B^*$	$A+2B^*\underset{k'_S}{\overset{k_R}{\rightleftharpoons}}R^*+L$	$R^*+\underset{k_R}{\overset{k'_R}{\rightleftharpoons}}R+L$		
VI	$A+L\underset{k'_A}{\overset{k_A}{\rightleftharpoons}}A^*$	$A^*+2B\underset{k'_S}{\overset{k_S}{\rightleftharpoons}}R^*$	$R^*\underset{k_R}{\overset{k'_R}{\rightleftharpoons}}R+L$		
VII	$A+L\underset{k'_A}{\overset{k_A}{\rightleftharpoons}}A^*$	$B+L\underset{k'_B}{\overset{k_B}{\rightleftharpoons}}B^*$	$A^*+B\underset{k'_C}{\overset{k_C}{\rightleftharpoons}}C^*$	$C^*+B^*\underset{k'_S}{\overset{k_S}{\rightleftharpoons}}R^*+L$	$R^*\underset{k_R}{\overset{k'_R}{\rightleftharpoons}}R+L$
VIII	$A+L\underset{k'_A}{\overset{k_A}{\rightleftharpoons}}A^*$	$2B+2L\underset{k'_B}{\overset{k_B}{\rightleftharpoons}}2B^*$	$A^*+B^*\underset{k'_D}{\overset{k_D}{\rightleftharpoons}}D^*+L$	$D^*+B^*\underset{k'_S}{\overset{k_S}{\rightleftharpoons}}R^*+L$	$R^*\underset{k_R}{\overset{k'_R}{\rightleftharpoons}}R+L$
IX	$A+L\underset{k'_A}{\overset{k_A}{\rightleftharpoons}}A^*$	$A^*+B\underset{k'_C}{\overset{k_C}{\rightleftharpoons}}C^*$	$C^*+B\underset{k'_S}{\overset{k_S}{\rightleftharpoons}}R^*$	$R^*\underset{k_S}{\overset{k'_S}{\rightleftharpoons}}R+L$	
X	$B+L\underset{k'_B}{\overset{k_B}{\rightleftharpoons}}B^*$	$B^*+A\underset{k'_C}{\overset{k_C}{\rightleftharpoons}}C^*$	$C^*+B\underset{k'_S}{\overset{k_S}{\rightleftharpoons}}R^*$	$R^*\underset{k_R}{\overset{k'_R}{\rightleftharpoons}}R+L$	
XI	$A+L\underset{k'_A}{\overset{k_A}{\rightleftharpoons}}A^*$	$H_2+2L\underset{k'_H}{\overset{k_H}{\rightleftharpoons}}2H^*$	$A^*+2B^*\underset{k'_S}{\overset{k_S}{\rightleftharpoons}}D^*+2L$	$D^*+H_2\underset{k'_D}{\overset{k_D}{\rightleftharpoons}}R^*$	$R^*\underset{k_R}{\overset{k'_R}{\rightleftharpoons}}R+L$
XII	$A+L\underset{k'_A}{\overset{k_A}{\rightleftharpoons}}A^*$	$2H_2+4L\underset{k'_H}{\overset{k_H}{\rightleftharpoons}}4H^*$	$A^*+2H^*\underset{k'_S}{\overset{k_S}{\rightleftharpoons}}D^*+2L$	$D^*+2B^*\underset{k'_D}{\overset{k_D}{\rightleftharpoons}}R^*+2L$	$R^*\underset{k_R}{\overset{k'_R}{\rightleftharpoons}}R+L$
XIII	$H_2+2L\underset{k'_H}{\overset{k_H}{\rightleftharpoons}}2H^*$	$S+2H^*\underset{k'_D}{\overset{k_D}{\rightleftharpoons}}D^*+L$	$D^*+H_2\underset{k'_S}{\overset{k_S}{\rightleftharpoons}}R^*$	$R^*\underset{k_R}{\overset{k'_R}{\rightleftharpoons}}R+L$	

In Table 4, A stands for carbon monoxide; B, hydrogen molecule; H, hydrogen atom; C and D, intermediate products; R, methanol; L, active site, and superscript*, activated state. The symbols k_i's and k_i's are the rate constants for the forward and reverse reactions where i=A, B, C, D, H, R, and S.

ing step, all four steps are examined one after another eliminating those which conflict with the experimental data. The examining procedure is explained by picking, for instance, step c as the rate determining step. We then express the rate equations for all four steps, and equate all four rates to zero at equilibrium obtaining the concentration of free active sites, C_L, on the catalyst by:

$$C_L = \frac{C_{Lo}}{1+K_A P_A + \sqrt{K_B P_B} + K_R P_R} \quad (4)$$

where C_{Lo} is the initial active site concentration, K_A, K_B, and K_R are the equilibrium constants for reaction 3a, 3b, and 3d, respectively. The use of steady state assumption leads to an equality of all four rates r_A, r_B, r_S, and r_R, and the use of Eq. (4) enables us to derive the final rate equation for the overall reaction as follows:

$$r = \frac{P_A P_B^2 - P_R/K}{(\alpha+\beta P_A+\gamma P_B+\delta P_R)^3} \quad (5)$$

where K is the equilibrium constant for reaction (2) which is equal to $p_R/p_A p_B^2$, and α, β, γ, and δ are all positive constants that depend only on temperature. The above equation can be rewritten in the following form:

$$\sqrt[3]{\frac{P_A P_B^2 - P_R/K}{r}} = \alpha+\beta P_A+\gamma p_B+\delta P_R \quad (6)$$

Similar procedures are followed by taking each of the re maining steps as the rate controlling step. and equations similar to Eq. (6) are obtained. The permissible rate determining step is the one which gives a set of non-negative coefficients, α, β, γ, and δ.

In the mechanism just shown, we assumed that there are four reactions taking place. Examination proved that the four coefficients are all positive only when step 3c was taken as the rate determining step while other steps did not produce all positive coefficients. However, it may be possible to find some other rate determining steps by assuming different reaction mechanisms. The trial reaction mechanisms examined in this work are listed in Table 4. Only five mechanisms out of thirteen gave sets of positive coefficients as shown in Table 5, and other mechanisms failed in meeting this requirement. In principle, we could pick any of the five qualified mechanisms. However, we wish to draw a single answer. Under the given situation, there seems to be no other methods of narrowing down the answer but to choose a rate equation which best fit the data. In the last column of Table 5, we have shown the values of standard deviation of the observed rates from the calculated ones. Inspection of this table will tell us that mechanism IIc shows a least deviation, followed by Ic. We will primarily use mechanism IIc for the reactor simulation, but, the others will also be used for the purpose of comparison.

When we inspect the reaction mechanisms in Table 4 and the rate expressions in Table 5, we find that the rate determining steps, Ic, IIc, and IIIc are the steps where surface reactions between adsorbed molecules or atoms are taken place. On the other hand, in steps IVa and Va, surface adsorption controls the rate, and in steps IVb and Vb, reactions between surface and gas phase control the rate of the overall reaction. At any rate, the best data fit is obtained in reaction mechanism IIc, and it is followed by in the order of Ic, IIIc, IVa, Va, Vb, and IVb. This order, however, may not be a very important criterion in sorting the best answer.

REACTOR MODELLING AND SIMULATION

The reactor we have to deal with is a completely specified plant-scale catalytic reactor at specified reaction conditions. The reactor, catalyst, and process conditions are well described in Table 2, and the physical propeties and thermodynamic information are given in Table 3. Since our reactor model can be decribed as a simple, one-dimensional, plug-flow, pseudo-homogeneous, non-isothermal reactor, we can assume that there is no axial and radial diffusion and the distribution of voidage in the catalyst bed is uniform. Let us consider an elemental length of the catalyst bed, Δz as shown in Fig. 1. We will set up balance equations regarding to this elemental length of the catalyst bed in reference to various source of information[5,6,7,8, and 9].

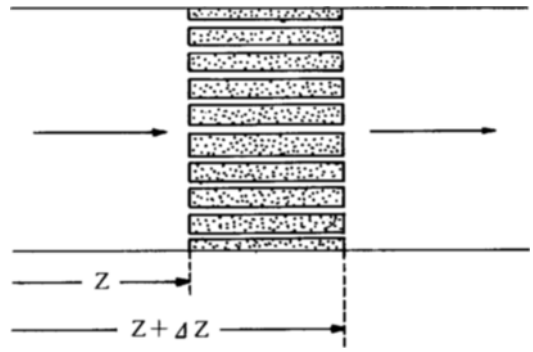

Fig. 1. Reactor Tube Element Filled with Catalyst

Mass Balance If the cross-sectional area of the reactor tube is denoted by S, molar flow rate of B per cross-sectional area of tube, by N_B, and the rate of generation of B based on reactor volume, by R_B, the mass balance equation will be as follows:

$$SN_B|_z - SN_B|_{z+\Delta z} + R_B S\,\Delta z = 0 \quad (7)$$

But, as Δz is approached to zero, Eq. (7) can be reduced to:

Table 5. Rate Equations and the Values of Coefficients for Various Reaction Mechanisms

Rx. Mech.	Rate Equation	Temp. °K	α	β	γ	δ	Std. Dev.
Ic	$\sqrt[3]{\frac{p_A p_B^2 - p_R/K}{r}} = \alpha + \beta p_A + \gamma p_B + \delta p_R$	475	5.001	0.5255	0.2167	0.9382	0.1350
		485	6.161	0.3925	0.1715	0.5896	0.1327
		495	3.564	0.3265	0.1520	0.4663	0.4026
IIc	$\sqrt[5]{\frac{p_A p_B^2 - p_R/K}{r}} = \alpha + \beta p_A + \gamma p_B^{\frac{1}{2}} + \delta p_R$	475	2.263	0.1717	0.4969	0.1273	0.0858
		485	2.256	0.0580	0.4408	0.0875	0.1596
		495	1.633	0.0531	0.4151	0.0752	0.3045
IIIc	$\sqrt[3]{\frac{p_A p_B^2 - p_R/K}{r}} = \alpha + \beta p_B^{\frac{1}{2}} + \gamma p_A p_B + \delta p_r$	475	18.19	0.3098	0.0072	0.9382	0.1483
		485	13.70	0.5356	0.0056	0.5890	0.1324
		495	10.55	0.4817	0.0045	0.4662	0.5379
IVa	$\sqrt[4]{\frac{p_A p_B^2 - p_R/K}{r}} = \alpha p_A^{\frac{1}{4}} + \beta p_R^{\frac{1}{4}} + \gamma p_R p_A^{\frac{1}{4}}$	475	6.385	0.0101	0.1237		0.4423
		485	5.318	0.4041	0.0687		0.6902
		492	4.601	0.2616	0.610		1.7140
IVb	$\sqrt[4]{\frac{p_A p_B^2 - p_R/K}{r}} = \alpha + \beta p_B^{\frac{1}{2}} + \gamma p_R$	475	5.253	1.0810	0.2777		1.0210
		485	4.733	0.9148	0.1752		1.4050
		495	3.503	0.8463	0.1537		3.4860
Va	$\sqrt{\frac{p_A p_B^2 - p_R/K}{r}} = \alpha p_A^{\frac{1}{2}} + \beta p_A^{\frac{1}{2}} p_R + \gamma p_R^{\frac{1}{2}}$	475	40.49	1.7710	0.2692		0.4361
		485	30.23	0.9476	0.6086		0.6883
		495	21.85	0.6554	1.6740		1.7040
Vb	$\sqrt{\frac{p_A p_B^2 - p_R/K}{r}} = \alpha + \beta p_B + \gamma p_R$	475	5892	2.0830	9.0860		0.9821
		485	54.58	1.4090	4.7900		1.3810
		495	30.18	1.1750	3.6510		3.3590

Note: The standard deviation here is with respect to the rate equation as given by Eq. (5), not by Eq. (6) of the text.

$$\frac{dN_B}{dz} = R_B \tag{8}$$

On the other hand, it can be shown that combination of ideal gas law and the concept of catalyst voidage will yield the following relations:

$$P_B \varepsilon V_e = N_B RT \tag{9}$$

where V_e is the linear velocity through the void space. This equation can alternately be expressed in the following form:

$$N_B = \frac{\varepsilon P_B V_e}{RT} \tag{10}$$

Differentiating the both sides with respect to z, and combining with Eq. (8), we obtain:

$$TP_B \frac{dV_e}{dz} + TV_e \frac{dP_B}{dz} - P_B V_e \frac{dT}{dz} = \frac{RT^2}{\varepsilon} R_B \tag{11}$$

Energy Balance In setting up the energy balance equation, we neglect the mechanical energy terms and assume a uniform flow and heat generation by reaction over the catalyst bed cross section. Then we can write that the heat output minus heat input equals to the heat generation minus heat loss, or, in mathematical expression, as follows:

$$CSN(T-T_d)|_{z+\Delta z} - CSN(T-T_d)|_z = R_R(-\Delta H_p)S\,\Delta z - \pi D\,\Delta z U(T-T_w) \tag{12}$$

where C is the average molar heat capacity, N, total molar flow rate per unit cross-sectional area of the tube, T_d, the reference temperature, R_R, molar rate of generation of product R per unit catalyst volume and time, T_w, the wall or coolant temperature, $-\Delta H_p$, heat of reaction per mole of R, D, diameter of the tube, U, heat transfer coefficient between the reacting zone and the coolant fluid.

As Δz is approached to zero, Eq. (12) will become:

$$CS\frac{d}{dz}[N(T-T_d)] = R_R(-\Delta H_P)S - \pi DU(T-T_w) \tag{13}$$

Differentiating the left side term, and by letting $T_d = 0$, we will obtain:

$$\frac{d}{dz}[N(T-T_d)] = N\frac{dT}{dz} + T\frac{dN}{dz} \tag{14}$$

Since $N = N_A + N_B + N_R$, and if their initial values are denoted by N_{Ao}, N_{Bo}, and N_{Ro} (=0),

$$N = N_B + N_{Ao} \tag{15}$$

Therefore,

$$\frac{dN}{dz} = \frac{dN_B}{dz} \tag{16}$$

and Eq. (14) will become:

$$\frac{d}{dz}[N(T-T_a)] = (N_B+N_{Ao})\frac{dT}{dz} + T\frac{dN_B}{dz} \quad (17)$$

So, it follows from Eqs. (13) and (17) that:

$$(N_B+N_{Ao})\frac{dT}{dz} + \frac{dN_B}{dz} = \frac{(R_R)(-\Delta H_P)}{C} - \frac{\pi DU(T-T_W)}{CS} \quad (18)$$

Introducing $N_B = P_B V_e \varepsilon/(RT)$, $N_{Ao} = P_{Ao} V_{eo} \varepsilon/(RT_o)$ and Eq. (8) into Eq. (18) and rearranging the resulting equation, we obtain:

$$\frac{dT}{dz} = \left[\frac{R_R(-\Delta H_P)}{C} - \frac{\pi DU(T-T_W)}{CS} - TR_B\right] \left[\frac{P_B V_e \varepsilon}{RT} + \frac{P_{Ao} V_{eo} \varepsilon}{RT_o}\right]^{-1} \quad (19)$$

Momentum Balance It is clear that the mass rate of flow in the reactor tube is constant at steady state. But, the linear velocity of the fluid through the void space varies. Therefore, there is changes in the rate of mometum flow across the catalyst element $(\frac{1}{2}D)^2\Delta z$. This means that any force applied axially to the catalyst element is responsible partially for increasing the rate of momentum flow, and partially for overcoming the friction in the void space. Therefore, the momentum balance can be written as in the following mathematical expression;

$$-S_e dP = w dV_e + \tau dA_P \quad (20)$$

where w is the mass rate of flow, p, total pressure, τ, shear stress at the catalyst surface, A_p, surface area of the catalyst.

Dividing through the both sides by dz, and rearranging the resulting equation, we obtain:

$$\frac{dP}{dz} = \frac{w}{S_e}\frac{dV_e}{dz} - \frac{\tau}{S_e}\frac{dA_P}{dz} \quad (21)$$

The second term of the right hand side of Eq. (21) is the pressure drop term due to the friction in the void space, and it can be written as:

$$\left(\frac{dP}{dz}\right)_f = \left(-\frac{\tau}{S_e}\right)\frac{dA_P}{dz} \quad (22)$$

According to Leva [10], the right hand side term can be replaced by:

$$\left(\frac{dP}{dz}\right)_f = \frac{4f_m(1-\varepsilon)^{3-n}}{\phi_s^{3-n}\varepsilon^3 D_P}\frac{U_o^2}{2g_c} \quad (23)$$

where f_m and n are the functions of Reynolds number, $D_p V_e \rho/\mu$, based on particle diameters, ϕ_s, shape factor of the solid particles, U_o, the fluid superficial velocity which equals to εV_e here, and g_c, the conversion factor of mass into force (but, in our case this is taken as 1).

On the other hand, the total pressure of the system can be expressed, using Eq. (15), as follows:

$$P = \frac{RT}{V_e}(N_B+N_{Ao}) = \frac{RT}{V_e}\left(\frac{\varepsilon V_{eo}}{RT_o}P_{Ao} + \frac{\varepsilon V_e}{RT}P_B\right) \quad (24)$$

Differentiating Eq. (24) with respect to z, we obtain:

$$\frac{dP}{dz} = \frac{V_{eo}P_{Ao}}{T_o}\left(\frac{1}{V_e}\frac{dT}{dz} - \frac{T}{V_e^2}\frac{dV_e}{dz}\right) + \frac{dP_B}{dz} \quad (25)$$

Combining Eqs. (21), (23) and (25) we arrive at:

$$\frac{dP_B}{dz} + \frac{V_{eo}P_{Ao}}{T_o}\left(\frac{1}{V_e}\frac{dT}{dz} - \frac{T}{V_e^2}\frac{dV_e}{dz}\right) = -\frac{w}{S_e}\frac{dV_e}{dz} - \frac{2f_m(1-\varepsilon)^{3-n}}{\phi_s^{3-n}\varepsilon D_P}\frac{w}{S_e}V_e \quad (26)$$

Modelling Summary Equations (11), (19), and (26), each derived from considering mass, energy, and momentum balances, provide us a set of simultaneous first order non-linear ordinary differential equations which must be solved with the boundary conditions as given below;

$$\begin{aligned} T &= T_o && \text{at } z=0 \\ P_B &= P_{Bo} && \text{at } z=0 \\ V_e &= V_{eo} && \text{at } z=0 \end{aligned} \quad (27)$$

The solution can best be obtained numerically by using the semi-implicit Runge-Kutta method. For this purpose, we rewrite the equations by defining new functions such that:

$$f_1 = \left[\frac{R_R(-\Delta H_P)}{C} - \frac{DU(T-T_W)}{CS} + 2TR_R\right] \left[\frac{P_B V_e \varepsilon}{RT} + \frac{P_{Ao} V_{eo} \varepsilon}{RT_o}\right]^{-1} \quad (28)$$

$$f_2 = -\frac{2f_m(1-\varepsilon)^{3-n}}{\phi_s^{3-n}\varepsilon D_P}\frac{w}{S_e}V_e \quad (29)$$

$$f_3 = -2T^2R_R/(\varepsilon/R) + P_B V_e f_1 - TV_e\left(f_2 - \frac{P_{Ao}V_{eo}}{T_o}\frac{f_1}{V_e}\right) \quad (30)$$

$$f_4 = TP_A - \frac{w}{S_e}TV_e + \frac{P_{Ao}V_{eo}}{T_o}\frac{T^2}{V_e} \quad (31)$$

$$f_5 = \left(-2\frac{R}{\varepsilon}T^2R_R + P_B V_e f_1 - TP_B\frac{f_3}{f_4}\right)/(TV_e) \quad (32)$$

Then, the three differential equation will become as follows:

$$\frac{dT}{dz} = f_1 \quad (33)$$

$$\frac{dV_e}{dz} = \frac{f_3}{f_4} \quad (34)$$

$$\frac{dP_B}{dz} = f_5 \quad (35)$$

with boundary conditions as in Eq. (27).

The actual solving procedure is to calculate the f_i's using the initial values of the variables followed by integration which will generate the next values to be plugged into the f-functions. This procedure is repeated until the end of the reactor tube is reached[11].

RESULTS

The results of computer simulation for reactor performance using different reaction mechanisms were plotted and tabulated comparatively. It is hoped, from this comparison, to find some substantial clue to deciding which one of the reaction mechanisms is more justifiable than deciding by the magnitude of standard deviation.

The reaction temperature, pressure, and concentration profiles are shown in Fig. 2, 3, and 4 for reaction mechanisms Ic and IIc. Shown in Fig. 5 are the temperature profiles for reaction mechanisms IIIc, IVa, and Va, and in Fig. 6, the reaction rate profiles for reaction mechanisms Ic, IIc, IIIc, IVa, IVb, Va, and Vb.

On the other hand, the summaries of reactor performance were tabulated in the prescribed format in Tables 6 and 7.

DISCUSSION

It was shown in Tables 4 and 5 that the seven rate determining steps of the five reaction mechanisms were

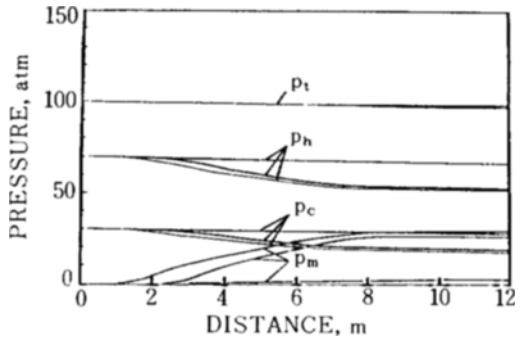

Fig. 3. Plots of Total Pressure and Partial Pressures for Hydrogen, Carbon Monoxide, and Methanol for Reaction Mechanism IIc. The Upper, Middle and Lower Curves are for Shell Side Temperatures of 473, 483, and 493°K, respectively. But, in the Case of Methanol, the Order is Reversed.

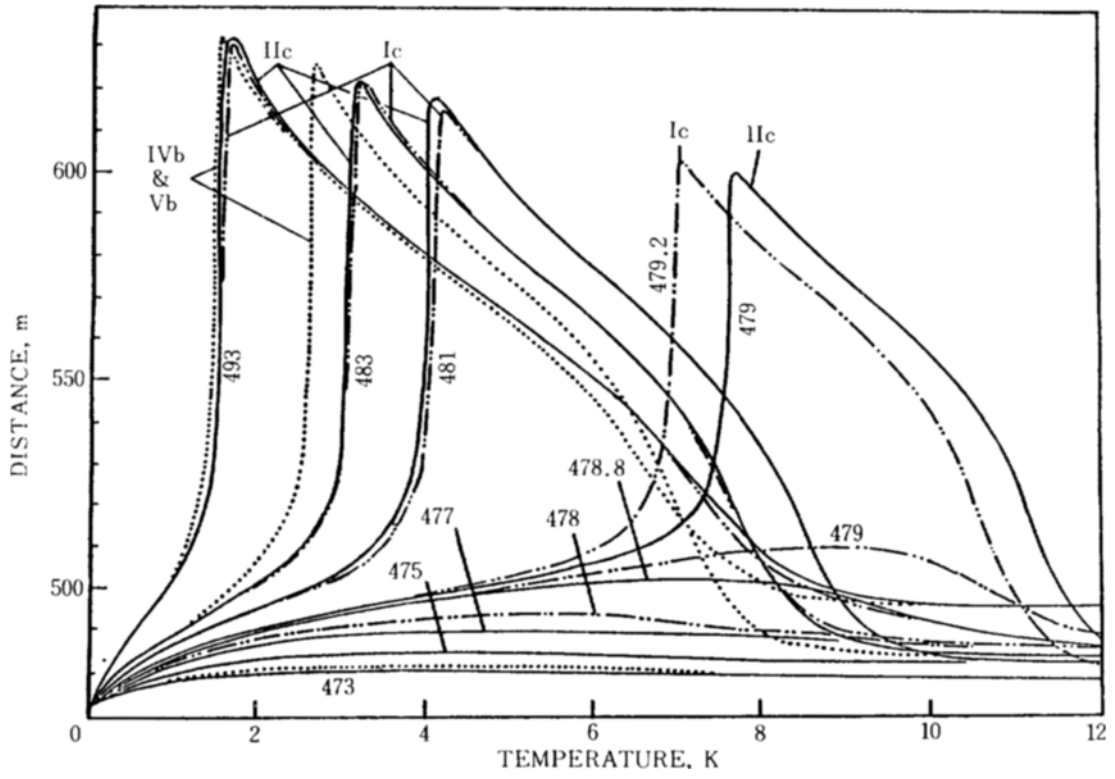

Fig. 2. Reactor Bed Temperature versus Distance in Tube for Reaction Mechanisms Ic, IIc, IVb, and Vb, Showing the Occurrence of Hot Points

Table 6. Results of Simulation for Reaction Mechanisms Ic and IIc

Rx. Mech.	Description	Calculated Values								
Ic	Shell Side Temperature, °K	473	475	477	478	479	479.2	481	483	493
	Max. Tube side Temp., °K	480.96	485.00	490.34	494.35	510.51	603.61	617.90	622.99	632.44
	Location from Inlet of Max. Temp. m	4.20	4.20	4.80	5.40	9.03	7.04	4.14	3.16	1.64
	Outlet Temperature, °K	479.14	482.14	485.15	486.46	488.54	483.27	482.47	484.66	496.28
	Outlet Methanol Concentration, mol/m^3	79.32	96.52	122.12	142.86	255.66	632.26	649.68	658.65	701.42
	Fraction of Equil. Value	0.0018	0.0026	0.0040	0.0051	0.0119	0.0399	0.0402	0.0466	0.0992
	Production Rate, x10^{4}kg/hr	1.7615	2.1281	2.6566	3.0679	5.0885	9.9475	10.107	10.225	10.806
IIc	Shell Side Temperature, °K	473	475	477	478	478.8	479	481	483	493
	Max. Tube side Temp., °K	480.95	485.03	490.47	494.70	502.99	600.33	618.11	623.05	632.37
	Location from Inlet of Max. Temp., m	4.20	4.20	4.80	5.40	6.90	7.68	4.08	3.14	1.64
	Outlet Temperature, °K	479.17	482.19	485.24	486.55	486.85	488.67	482.46	484.66	496.32
	Outlet Methanol Concentration, mol/m^3	79.38	96.95	123.45	145.62	195.57	627.53	655.49	664.48	708.30
	Fraction of Equil. Value	0.0018	0.0026	0.0041	0.0053	0.0077	0.0526	0.0410	0.0475	0.1017
	Production Rate, x10^{4}kg/hr	1.7628	2.1372	2.6834	3.1213	4.0461	9.9728	10.166	10.284	10.873

proved compatible with supplied experimental data. However, the step that was considered as the most plausible one had been chosen based on the least standard deviation. Fig. 2 shows that the temperature profile of reaction mechanism Ic nearly coincide with that of reaction mechanism IIc if the reactor wall temperature is kept the same.

The most striking behavior of all is an abrupt jump exhibited by some temperature profiles at around 479 °K of wall temperature. For instance, in the case of reaction mechanism IIc, this jump occurs at 479 °K, and in reaction mechanism Ic, at 479.2 °K, while until up to temperatures different from these temperatures only by 0.2 °K the profiles form very slowly rising and then falling curves. After the incipient jump, the profiles take gradual downward slopes approaching towards the wall temperature at the end of the reactor tube. Furthermore, the higher the wall temperature, the earlier and the higher the jump occurs in the reactor tube. One will note that the effect of the jump can easily be recognized even in the plots of reactor pressure, molal flow rate,

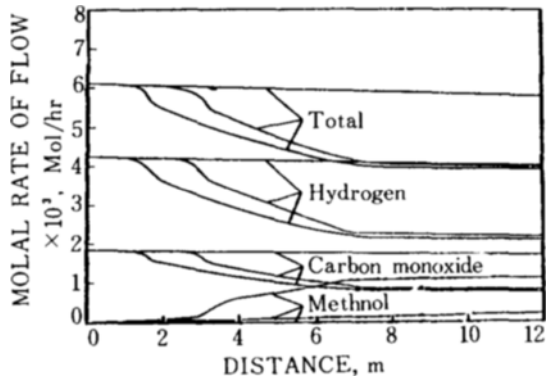

Fig. 4. Plots of Molal Rate of Flow versus Distance for Total Gas Mixture, Hydrogen, Carbon Monoxide, and Methanol for Reaction Mechanism IIc. The Upper, Middle, and Lower Curves are for Shell Side Temperatures of 473, 483 and 493°K, respectively. But, in the Case of Methanol, the Order is Reversed.

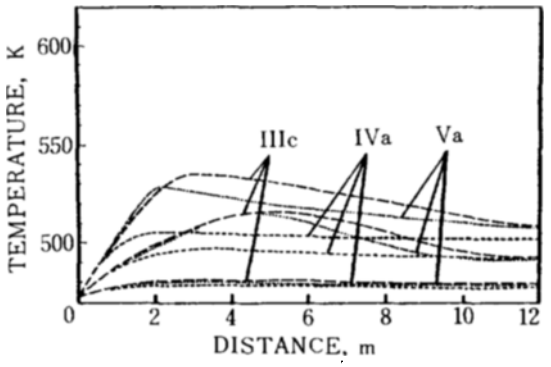

Fig. 5. Reactor Bed Temperature versus Distance in Tube for Reaction Mechanisms IIIc, IVa, and Va, Showing no Hot Point Occurrence. The Uppermost Curves are for Shell Side Temperature of 493°K, and the Middle and Lower Curves are for Those of 483 and 473°K respectively.

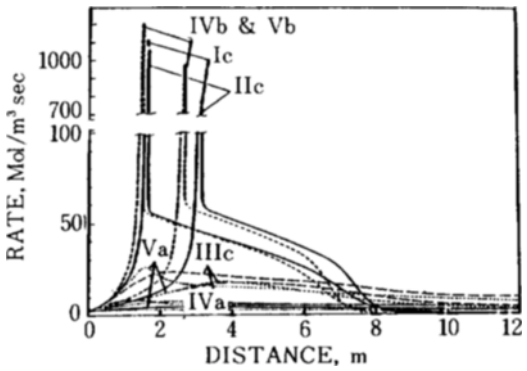

Fig. 6. Reaction Rate versus Distance in Tube for Reaction Mechanisms Ic, IIc, IIIc, IVa, IVb, Va, and Vb, Each for Three Different Shell Side Temperatures of 493, 483 and 473 °K from the Upper, Middle and Then to the Lower Profiles

and reaction rate profiles in Fig. 3, 4, and 6 at the corresponding locations.

Similar behaviors of temperature profiles for reaction mechanisms IVb and Vb can be observed in Fig. 2. The location at which this jump occurs in the tube may be called a "hot point". The existance of a hot point may or may not be desirable depending on the stoutness of the catalyst. Perhaps, an abrupt rise in temperature may cause undesirable reactions, or impare the catalyst. Therefore, in most cases, creation of an uneven temperature profile may have to be avoided.

Mechanisms IVb and Vb give almost superimposable temperature profiles upon each other. But, they are slightly dislocated from the profiles for reaction mechanisms Ic and IIc. However, mechanisms IIIc, IVa, and Va, whose temperature profiles are shown in Fig. 5, do not exhibit a jump at temperatures below 493 °K, the upper limit of wall temperature set. Even reaction mechanisms Ic and IIc do not show a jump at temperatures below 478.8 °K. The profiles form only small hills or plateaus.

In this respect we may rather wish to choose reaction mechanism IIIc which does not exhibit a hot point within the assigned range of wall temperature. This reaction mechanism holds the reactor temperature on relatively a high level enabling the reactor to operate at relatively a high rate of methanol production.

Shown in Table 6 is a summary of the detailed reactor performance computed for reaction mechanisms Ic and IIc, and in Table 7, an overall summary of the reactor performance for all possible reaction mechanisms except the ones just mentioned in order to provide a basis of comparison. It is obvious that mechanism IIc yields the best result in terms of the rate of methanol production so long as the catalyst activity is not hampered by the hot point temperature. However, if we

Table 7. Results of Simulation for Reaction Mechanisms IIIc, IVa, IVb, Va, and Vb

Description	Shell Side Temperature, °K								
	IIIc			IVa			IVb		
	473	483	493	473	483	493	473	483	493
Max. Tube Side Temperature, °K	481.2	516.0	535.0	478.8	497.0	505.4	482.3	625.0	632.8
Location from Inlet of Max. Temp., °K	4.2	4.8	3.2	3.6	3.6	2.4	3.6	2.7	1.5
Outlet Temperature, °K	479.3	492.0	507.6	477.6	491.9	502.1	479.2	484.5	495.9
Outlet Methanol Conc., mol/m^3	81.53	255.5	372.0	57.96	126.3	117.2	88.49	621.9	659.1
Fraction of Equilibrium Value, x10^{-3}	1.86	14.3	53.8	1.18	58.9	89.7	2.03	40.8	84.5
Production Rate, x10^{4}kg/hr	1.808	5.114	7.064	1.304	2.774	2.652	1.952	9.842	10.38

Description	Shell Temperature, °K					
	Va			Vb		
	473	483	493	473	483	493
Max. Tube Side Temperature, °K	480.0	515.1	528.4	482.2	625.4	633.2
Location from Inlet of Max. Temp., °K	3.6	4.5	2.1	3.6	2.7	1.5
Outlet Temperature, °K	478.2	490.5	507.2	479.1	484.5	495.9
Outlet Methanol Conc., mol/m^3	68.48	214.9	281.6	87.11	623.8	659.7
Fraction of Equilibrium Value, x10^{-3}	1.45	10.5	34.9	1.98	41.1	84.5
Production Rate, x10^{4}kg/hr	1.530	4.414	5.678	1.923	9.863	10.39

wish to stay aloof from the hot point hazard, adoption of reaction mechanism IIIc will be most desirable.

There is, however, no means of knowing whether the desired mechanism or a hot point mechanism is being followed. Only by an actual operating program of the reactor can the real mechanism be told.

CONCLUSION

In our kinetic analyses, we have exhausted almost all of the conceivable reaction models picking up only five permissible reaction mechanisms in which seven steps were considered to be the rate determining steps. The reactor simulation was carried out concentrating on mechanism IIc which yielded a least standard deviation of the data from the derived rate equation. Similar calculations were also carried out for the rest of the mechanisms in order not to miss any particularties that might be associated with the reactor behaviors. We found under the given assumption and reactor operating conditions that:

1. Surface reactions between the absorbed reactants or transitory compounds are the rate determining step in some mechanisms, one of which yielded a highest rate of methanol production.
2. The reaction between the active sites on the catalyst and a chemical component in the gas phase can also be the rate determining step, but, has no significant merits over the surface reactions.
3. Both the surface reactions and the surface-to-gas phase reaction mechanisms produce "hot points" in the reactor tube at wall temperatures beyond 478.8 °K at which the reaction rate rises abruptly and then falls gradually. The hot point temperature may possibly overheat that catalyst destroying its activity (reaction mechanisms IIc, Ic, IVb and Vb).
4. Among those reaction mechanisms which do not produce a hot point, one that involves a reaction between a transitory compound and adsorbed hydrogen gives a highest rate of methanol production, ranging approximately some 70% of that of hot point producing mechanisms.
5. It can not be decided which one of the steps permitted by the kinetic analyses will actually be followed without actually running the reactor and see the results. We can only tell which mechanism is of high yielding (10.873 x10^4 kg/hr of methanol) but dangerous, or safe but less productive (7.064 x 10^4 kg/hr of methanol).
6. Our prediction may not hold if the diffusion resistance were brought into consideration.

NOMENCLATURE

A : Carbon monoxide molecules

A_p : Surface area of catalyst particles, m^2

B : Hydrogen molecules

C : Molar heat capacity, 29.31 J/mol. °K

C_{LO} : Initial active site concentration

C_L : Free active site concentration

D : Reactor tube diameter, 3.81 x 10^{-2}m

D_p : Catalyst particle diameter, 7.87 x 10^{-3}m

f_1, f_2, f_3, f_4, f_5 : functions of T, V_e, P_B, and R_R

f_m : Friction coefficient in Leva's equation

$-\Delta H_p$: Heat of reaction at constant pressure per mole of methanol, 97.97 x 10^3 J/mol

k_A, k_B, k_s, k_R : Rate constants for forward reactions (3a), (3b), (3c), and (3d)

k_A', k_B', k_S', k_R' : Rate constants for backward reactions (3a), (3b), (3c), and (3d)

K_A, K_B, K_R : Equilibrium constants for reactions (3a), (3b), and (3d)

K : Equilibrium constant for reaction (2)

L : Active sites

N_A, N_B, N_R : Number of moles per unit time per unit cross-sectional area of the tube. N_{AO}, N_{BO}, and N_{RO} are their initial values

N : Total number of moles per unit time per unit cross-sectional area of the tube

P_A, P_B, P_R, or P_c, P_h, P_m : Partial pressures of carbon monoxide, hydrogen, and methanol, N/m^2

P_t : Total pressure of the reaction mixture, N/m^2

R : Gas constant, 8.314 J/mol. °K or methanol molecules

R_B, R_R : Rate of generation of hydrogen or methanol molecules per unit time and per unit catalyst volume, mol/m^3•sec

S, S_e : Cross-sectional areas of the reactor tube and void space, m^2

T_d, T_w, T_o, T : Reference temperature, shell side or wall temperature, initial temeprature, and temperature at any time or location in the tube, respectively

U, U_o : Overall heat transfer coefficient, J/m^2·sec. °K, and the fluid superficial velocity in Leva's equation

V_e, V_{eo} : Linear velocity through the void space at any location, and its value at the starting point, m/sec

w : Mass rate of flow, kg/sec

z : Distance from the inlet of the tube, m

Greek Letters

$\alpha, \beta, \gamma, \delta$: Coefficients of the rate equation

ϵ : Voidage

ϕ_s : Shape factor of solid particles

ρ : Density of the reaction mixture, kg/m^3

μ : Viscosity, Pa. sec

τ : Shear force at the wall, N

REFERENCES

(1) Nishtala, M.S., Berty, J.M. and Lee, S.: "Experimental Development in Kinetics and Catalysts", presented at the AIChE 75th Annual Meeting in Los Angeles, CA, November 14-19 (1982)

(2) Laidler, K.J.: "Kinetic Laws in Surface Catalysis", in "Catalysis", Vol. 1, edited by P.H. Emmett, Reinhold Publishing Corp., New York (1954).

(3) Natta, G.: "Synthesis of Methanol", in "Catalysis", Vol. 3, edited by P.H. Emmett, Reinhold Publishing Corp., New York (1956).

(4) Jenson, V.G. and Jeffreys, G.V.: "Mathematical Method in Chemical Engineering", 2nd Ed., Academic Press, Inc., New York (1977).

(5) Froment, G.F. and Bischoff, K.B.: "Chemical Reactor Analysis & Design", John Wiley & Sons (1979) p. 474.

(6) Smith, J.M. and Van Ness, H.C.: "Introduction to Chemical Engineering Thermodynamics", McGrow-Hill (1974), p. 449.

(7) Carberry, J.J.: "Chemical and Catalytic Reaction Engineering", McGrow-Hill (1976), p. 521.

(8) Gould, R.F.: "Chemical Reaction Engineering", 109, American Chemical Society (1972), p. 1.

(9) Petersen, E.E.: "Chemical Reaction Analysis", Prentice-Hall (1965), p. 175.

(10) Perry, R.H. and Chilton, C.H.: "Chemical Engineers Handbook", 5-52, 53, McGrow-Hill (1973).

(11) Villadsen, J. and Michelsen, M.L.: "Solution of Differential Equation Models by Polynomial Approximation", Prentice-Hall (1978), p. 317 and p. 417.